SCANNING VOL. 30, 365–380 (2008)

The Secondary Electron Emission Yield for 24 Solid Elements Excited by Primary Electrons in the Range 250–5000 ev: A Theory/Experiment Comparison

C.G.H. WALKER, M.M. EL-GOMATI, A.M.D. ASSA'D, and M. ZADRAŽIL

Department of Electronics, University of York, Heslington, York, United Kingdom

Summary: The secondary electron (SE) yield, δ, was measured from 24 different elements at low primary beam energy (250–5,000 eV). Surface contamination affects the intensity of δ but not its variation with primary electron energy. The experiments suggest that the mean free path of SEs varies across the d bands of transition metals in agreement with theory. Monte Carlo simulations suggest that surface plasmons may need to be included for improved agreement with experiment. SCANNING 30: 365–380, 2008. © 2008 Wiley Periodicals, Inc.

Key words: Monte Carlo, secondary electron yield, low energy, inelastic mean free path, d band

Introduction

The measurement and study of secondary electron emission (SEE) has a long history (McKay 1948; Baroody 1950; Dekker 1958). Secondary electrons (SEs) are regarded as those electrons, which were initially part of the valence or core levels of the material under the primary electron (PE) beam and have been excited to such an energy that they escape from the material. An SE is generally considered to be an electron, which exits the sample with an energy less than 50 eV. Although some SEs exit the sample with more than this energy and some backscattered PEs exit with less than 50 eV energy, the numbers are relatively small and 50 eV is a reasonably good threshold to distinguish the two types of electrons leaving the sample. McKay (1948) was the first person to notice that the maximum in the SEE yield, δ_m, was proportional to the work function (WF), φ. This may seem surprising as a higher WF implies a greater barrier for the electrons to escape from the surface. However Baroody (1950) determined that δ_m is proportional to $\varphi^{1/2}$ as a result of the SE generation process. This process includes the SE cascade whereby SEs collide with electrons within the material, which produce further SEs and so on. This process generates many more SEs than otherwise would have been the case.

The SE yield, δ, depends on the number of SEs generated as a function of depth, $n(z, E)$

$$n(z,E) = -\frac{1}{\epsilon}\frac{dE}{ds} \tag{1}$$

where ε is the energy required to produce a single SE and dE/ds is the stopping power. The SEs will be attenuated according to an exponential decay law. Hence, the total yield can be described by the equation:

$$\delta(E_{PE}) = \int n(z,E)\exp\left(-\frac{z}{\lambda}\right)dz \tag{2}$$

As discussed by Lin and Joy (2005), an analytical expression for the SE yield can be determined and is known as the "Universal Curve" that is given by

$$\frac{\delta}{\delta_m} = 1.28\left(\frac{E_{PE}}{E_{PE}^m}\right)^{-0.67} \times\left(1-\exp\left(-1.614\left(\frac{E_{PE}}{E_{PE}^m}\right)^{1.67}\right)\right) \tag{3}$$

where δ is the SE yield, δ_m is the maximum SE yield, E_{PE} is the primary beam energy and E_{PE}^m is the primary beam energy at which the maximum SE

Contract grant sponsor: Financial assistance was provided by the EPSRC

Address for reprints: Prof. M. M. El-Gomati, Department of Electronics, University of York, Heslington, York, YO10 5DD, UK, E-mail: mmg@ohm.york.ac.uk

Received 27 April 2008; Accepted with revision 4 June 2008

DOI 10.1002/sca.20124
Published online 25 July 2008 in Wiley InterScience (www.interscience.wiley.com)

yield occurs. Lin and Joy (2005) examine the SE yield curves with assistance of the Universal Curve to determine ε and the effective escape depth of the SEs, λ. However, the analysis carried out by Lin and Joy (2005) did not consider the SE cascade.

Barut (1954) pointed out that the curve of E_{PE}^{m} vs. atomic number is similar to the curve of density vs. atomic number. He also pointed out a relationship between δ_m and the density of the material and found a linear relationship between these two parameters for elements in the first half of each period (K to Co, and Rb to Ru).

Despite the long period of time that the SE yield has been studied, there remain considerable difficulties in describing its intensity and how it varies with PE energy. This is owing to the difficulty in understanding the properties of electrons at low energy (0–50 eV) such as the SE cascade and the knowledge of the inelastic mean free path (IMFP) at low electron energies.

A number of attempts to simulate the SE cascade have been reported using the Monte Carlo (MC) technique (Koshikawa and Shimizu 1973; Bongeler *et al*. 1993; Kuhr 1998; Kuhr and Fitting 1999; Ding *et al*. 2001; Ohya 2003; and Ziaja *et al*. 2005). This involves the modelling of the inelastic processes using the imaginary part of the dielectric function (in the case of Koshikawa and Shimizu 1974 an excitation function owing to Streitwolf 1959 is used). Using the theory of Penn (1987), the dielectric function can be used to determine the electron energy loss for each inelastic collision. For each energy loss of a PE, an SE is generated with the same energy as the energy lost by the PE. These SEs can then go on to generate further SEs in a cascade process. Ding *et al*. (2001) were able to show that the principal source of SEs leaving the sample is owing to the cascade process. Ding *et al*. (2001) used two methods of estimating the energy of the excited electron. First, they assumed that Fermi surface electrons dominated the contribution to the SE yield. This led to the equation:

$$E_s = E_F + \Delta E \tag{4}$$

where E_s is the energy of the SE, E_F is the Fermi energy and ΔE is the energy lost by the scattered electron. An improved method of determining E_s was suggested whereby the energy distribution of the valence electrons was taken into account. This led to the equation

$$E_s = E' + \Delta E \tag{5}$$

where E' is the initial energy of the valence electron. One drawback with using dielectric functions to determine the energy lost by the scattering electron, ΔE, is that the dielectric function is not available for all elements, so it would not be possible to simulate the SE process for all of the elements we have studied. In addition, the transport of electrons at energies between 1 and 50 eV is not well known and is known to be highly dependent on the band structure (Ziaja *et al*. 2006). This could result in considerable error in the MC simulation results. Hence, we have decided to only simulate the trajectory of the PEs by MC and use a simple direct line with exponential loss model to describe the SE transport and emission.

A database of all the SE yield results published to date has been published by Joy (2006). Inspection of the database reveals there is considerable scatter among the published SE yield measurements. The reason for the scatter is unclear but is probably related to the different sample preparation techniques and different instrumentation involved. By carrying out a series of experiments using modern equipment in ultra high vacuum (UHV) conditions, it is hoped that many of these variations can be eliminated. In this study, the SE yield of a total of 24 elements has been investigated in a systematic way, where the data are collected from both as inserted and ion cleaned surfaces under UHV. In addition, the PE range used is relevant to recent interest in low voltage scanning electron microscopy (LVSEM). Bronshtein and Fraiman (1969) also carried out a similar series of experiments on a considerable number of elements in a relatively good vacuum. Although Bronshtein and Fraiman (1969) is written in Russian and thus not easily accessible, many of the papers that form the basis of this work are available in English (e.g., Bronshtein and Brozdnichenko 1969; Bronshtein and Denisov 1965a,b; Bronshtein and Fraiman 1962a,b; Bronshtein and Segal 1960a, b). However, measurement techniques and theoretical understanding have advanced since that time and a new set of experiments may reveal new insights. In addition, although the results of Bronshtein and Fraiman (1969) cover a significant number of elements, the data reveal unphysical bumps and are rather sparse for some elements. The bumps could be owing to measurement errors or contamination. We will compare our results with those of Bronshtein and Fraiman (1969) in this report as well as the theoretical results of Ding *et al*. (2001).

This article is a continuation of the work reported in a companion paper (El-Gomati *et al*. (2008)). We should like to point out that the title of this companion paper and at various locations within that paper the term "backscattering factor" is used erroneously instead of the correct term "backscattering coefficient." "Backscattering factor" normally refers to the enhancement factor of an Auger peak $\neq$ signal owing to backscattered electrons.

Experiment

The experiment has already been described in the companion paper (El-Gomati *et al.* (2008)) and can also be found in the theses by Assa'd (1995) and Zadrazil (2002). We direct the reader who wishes to know more about the experimental procedure to these works. The elements studied in this report are: C (graphite), Al, Si, Ti, V, Cr, Fe, Ni, Cu, Ge, Zr, Nb, Mo, Ag, Cd, Sn, Gd, Hf, Ta, W, Pt, Au and Pb.

Results

The various SE yield measurements for all elements before and after cleaning are shown in Figures 1(a)–(x). In addition, the experimental results from Bronshtein and Fraiman (1969) and the theoretical results from Ding *et al.* (2001) are included in Figures 1(a)–(x) whenever available. The data acquired from the as-inserted samples are also shown in Figures 1(a)–(x) to show the SE yield that might be expected from an as-inserted specimen in a typical scanning electron microscopy (SEM). The data are shown in log–log form for two reasons. First, this form allows the data at low and high energy to be easily shown on a single graph without the low energy end being compressed. Second, the SE yield at high energy should approximately follow a straight line, which is principally defined by the stopping power at these energies (Reimer 1985, p 144). The data from each individual element will now be discussed in more detail.

Carbon

The results for carbon are shown in Figure 1(a). There is little change in δ after cleaning and there is good agreement between the present data and that of Bronshtein and Fraiman (1969).

Aluminum

The results for aluminum are shown in Figure 1(b). It was found that the value of δ increased considerably after cleaning. The increase in δ after cleaning for our sample suggests that the sample was initially coated with a thick layer of carbon like material that initially lowered δ. Ar cleaning was not able to remove the oxide, so δ increased at this stage. Our estimates for δ (after cleaning) as a function of PE energy agree with some other authors (e.g., Kanter 1961; Bruining and De Boer 1938; Shimizu 1974). However, it has been suggested that Kanter (1961) must have had a thin surface layer of Al_2O_3 contamination that resulted in a much higher value of δ (Bronshtein and Fraiman 1969, p 199). Bronshtein and Brozdnichenko (1969) have studied SEE from aluminum oxide and found that the much higher values of δ on the oxide as compared with the clean metal are owing to the much longer path length of SEs in the oxide. This leads to a greater volume from which SEs can escape into the vacuum, which in turn leads to a greater overall SEE. Thomas and Pattinson (1970) have determined δ at values lower than ours, but above those of Bronshtein and Fraiman (1969). Thomas and Pattinson (1970) used an evaporation technique and were able to take measurements within seconds after the end of the deposition. Hence, they were able to keep their sample relatively clean. The differences here could be owing to instrumental variations, but another possibility is that only Bronshtein and Fraiman (1969) have achieved a completely clean surface and all other authors (including ourselves) have a surface contaminated with oxygen to various degrees.

Silicon

The results for silicon are shown in Figure 1(c). On cleaning, δ increases but mostly for electrons with energies above 1 keV. δ from silicon is of considerable interest owing to the variations in δ with dopant concentration (El-Gomati and Wells 2001). It is also known that presence of oxygen on the surface of Si can influence the emission of electrons from the surface (Wagner and Spicer 1974). As it is known that our samples are likely to be oxidized, this may explain the difference between our results and those of Bronshtein and Fraiman (1969). Dionne (1975) employed Auger electron spectroscopy to determine the cleanliness of the Ar bombarded surfaces, but evidently still had oxygen contamination and thus the values of δ are also high. The theoretical calculations of Ding *et al.* (2001) agree well with the data of Bronshtein and Fraiman (1969).

Titanium

The results for titanium are shown in Figure 1(d). There is little change in the value of δ after cleaning. The present results are noticeably higher than those of Bronshtein and Fraiman (1969). A possible reason for this is the same as that for aluminum oxide—the mean free path of SEs is much higher in titanium oxide and our samples are slightly oxidized as determined from the backscattered electron yield (El-Gomati *et al.* 2008).

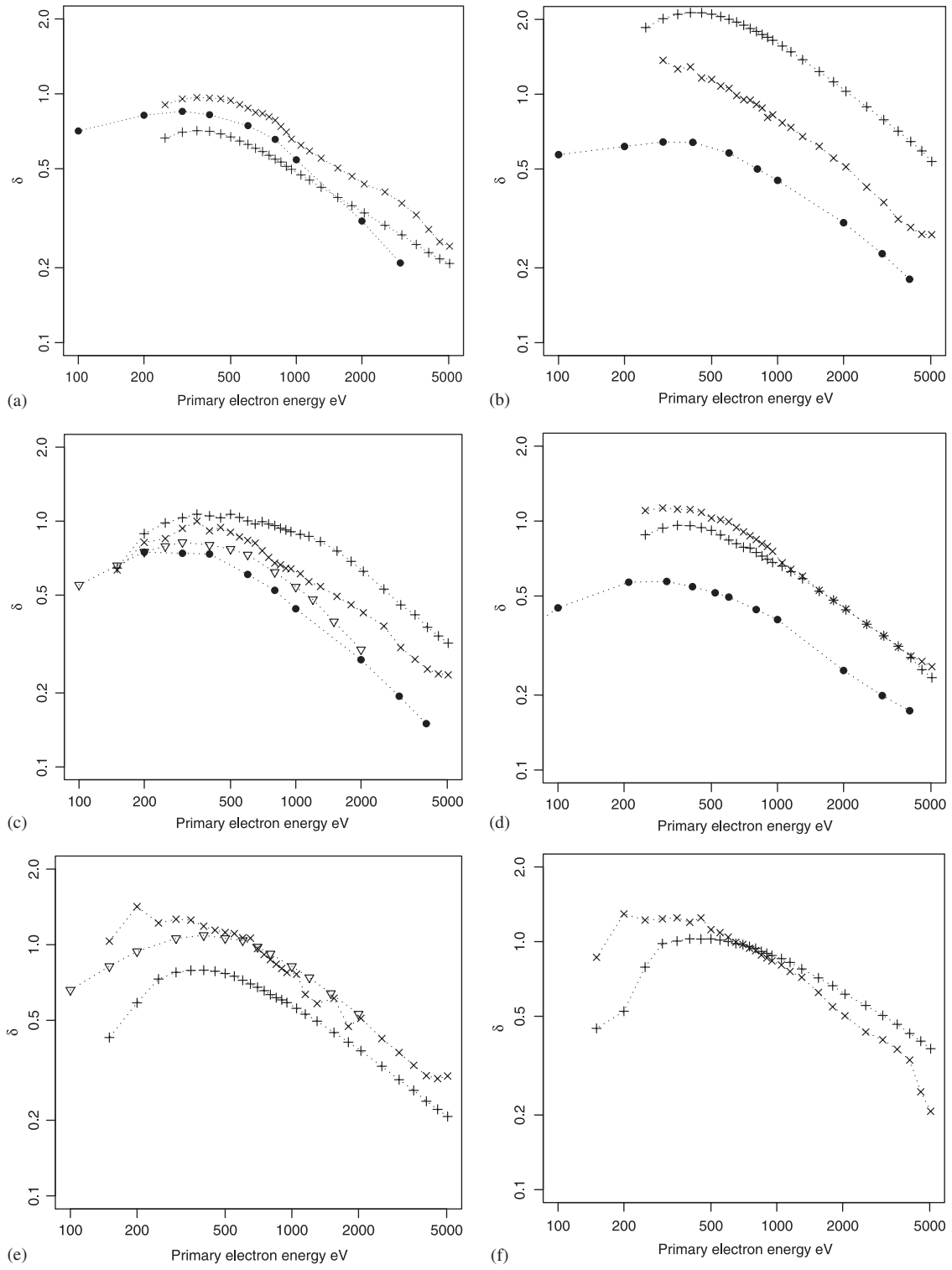

Fig 1. (a) The SE yield of carbon. The key for all figures in Figure 1 is as follows: x = as inserted sample, + = cleaned sample, ● = Bronshtein and Fraiman (1969). ∇ = Ding *et al.* (2001) using the method where the SE is assumed to come from a distribution of electron energies in the valence band (Equation (5)), Δ = Ding *et al.* (2001) using the method where the SEs are assumed to originate from the Fermi level (Equation (4)). The SE yield of (b) aluminum, (c) silicon, (d) titanium, (e) vanadium, (f) chromium, (g) iron, (h) nickel, (i) copper, (j) zinc, (k) germanium, (l) zirconium, (m) niobium, (n) molybdenum, (o) silver, (p) cadmium, (q) tin, (r) gadolinium, (s) hafnium, (t) tantalum, (u) tungsten, (v) platinum, (w) gold, (x) lead.

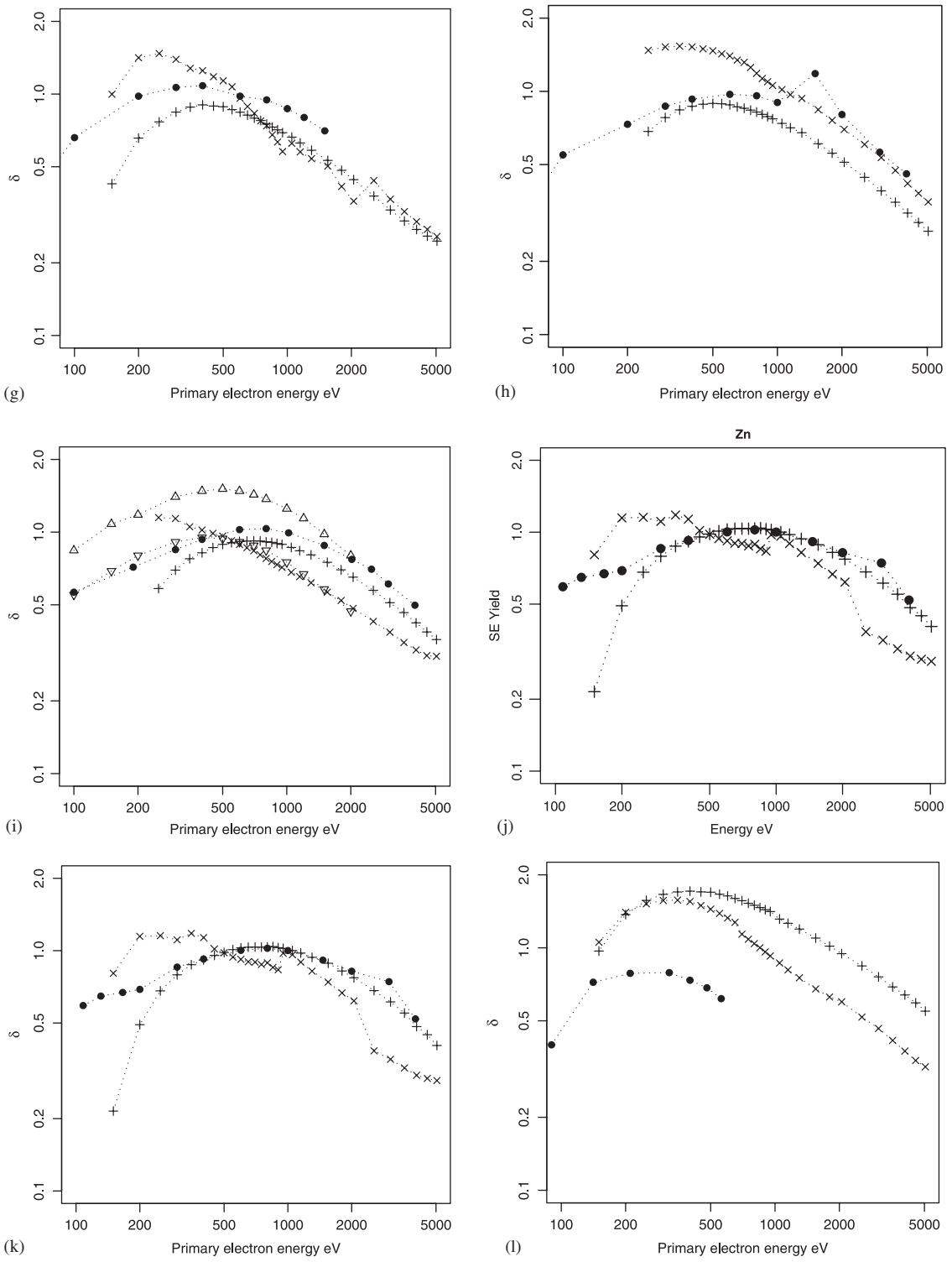

Fig 1. Continued.

Vanadium

The results for vanadium are shown in Figure 1(e). The value of δ drops after cleaning. There is reasonable agreement for the as-inserted data with the predictions of Ding *et al.* (2001) using the assumption that the SEs originate from the Fermi level. (Equation (4)). Ding *et al.* (2001) did not simulate vanadium using the assumption that electrons originate from a range of energies in the valence band (Equa-

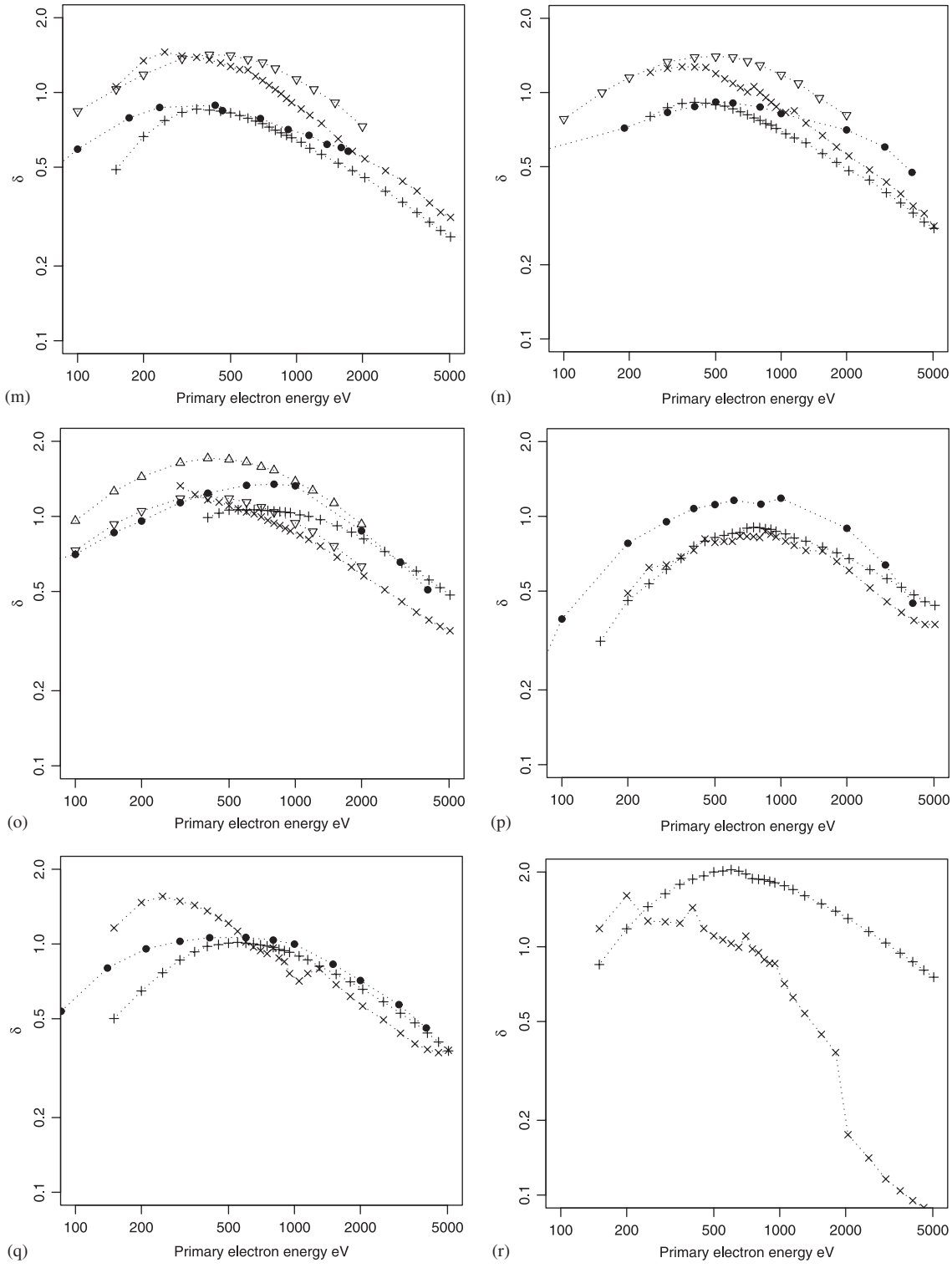

Fig 1. Continued.

tion (5)). Such a simulation may bring the theoretical results closer in to line with our measurements.

Chromium

The results for chromium are shown in Figure 1(f). The change in the value of δ after cleaning is only slight, but as with other elements, the curve is much smoother after cleaning.

Iron

The results for iron are shown in Figure 1(g). At high PE energy δ changes little on cleaning,

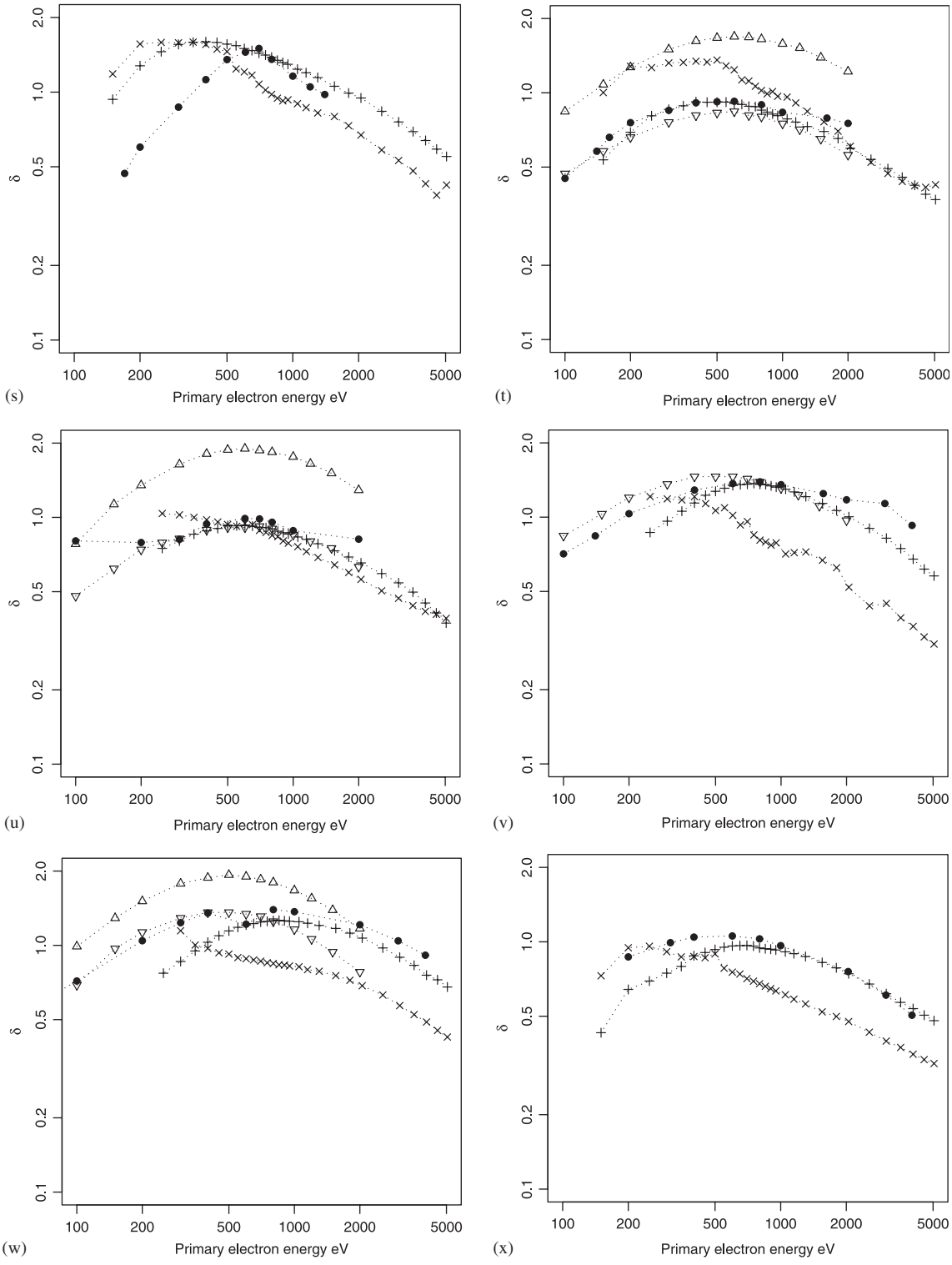

Fig 1. Continued.

whereas it drops after cleaning for low energies. Bronshtein and Fraiman (1969) obtain higher values of δ but the shape of the data from the cleaned sample and that of Bronshtein and Fraiman are quite similar.

Nickel

The results for nickel are shown in Figure 1(h). There is a slight drop in δ on cleaning. Our results are in good agreement with Bronshtein and Fraiman

(1969) at low PE energy but at higher PE our results are slightly lower than these authors who are also lower than the majority of other results on this metal (Thomas and Pattinson 1969; Luo *et al*. 1991; Whetten 1962) (not shown in the figure for reasons of clarity). In addition, the data from Bronshtein and Fraiman (1969) show a peak at around 1500 eV, which is unexplainable, but indicative of behavior from as inserted surfaces obtained in this study.

Copper

The results for copper are shown in Figure 1(i). δ increases slightly after cleaning for high PE energy, but drops slightly for the lowest PE energies. Relatively good agreement is found between the data presented here for the as-inserted data and that of Bronshtein and Fraiman (1969) and Shimizu (1974). The theoretical calculations of Ding *et al*. (2001) where the assumption is made that the Fermi level is the principal source of valence electron energies as the initial energy of the SE (Equation (4)) overestimates the intensity of the SEE, whereas assuming that the SE originates from a distribution of energies in the valence band (Equation (5)) results in better agreement.

Zinc

The results for zinc are shown in Figure 1(j). δ increases slightly after cleaning for high PE energy, but reduces for the lowest PE energies. Relatively good agreement is found between the data presented here from the cleaned samples and those of Bronshtein and Fraiman (1969).

Germanium

The results for germanium are shown in Figure 1(k). δ increases slightly after cleaning for high PE energy, but reduces for PE energies below 1 keV. The maximum in δ occurs at a higher energy (i.e., $E_{\mathrm{PE}}^{\mathrm{m}}$) for the data we acquired in comparison with Bronshtein and Fraiman (1969), but the intensity of the maximum, δ_{m}, is much the same. Our data from the as-inserted samples is somewhat similar to that given by Johnson and McKay (1954). These authors did not employ *in-situ* cleaning or *in-situ* evaporation, and hence their surfaces were probably contaminated. This gives re-assurance that the cleaned data presented here are of pure Ge.

Zirconium

The results for zirconium are shown in Figure 1(l). The value of δ increases after cleaning particularly at high PE energy. The present data for Zr are greater in value than that obtained by Bronshtein and Fraiman (1969). From the backscattering data, we know our samples were contaminated with a layer of oxygen. This is probably the reason for the discrepancy between the two results. It was considered that the oxide has a similar effect as it does in aluminum, namely that the IMFP of the SEs in zirconium oxide is much longer than in zirconium metal. However, if the IMFP of the SEs was much longer, this ought to move the PE energy where the maximum yield occurs (i.e., $E_{\mathrm{PE}}^{\mathrm{m}}$) to a higher energy (see later section entitled "Monte Carlo"). However, this does not seem to occur and indeed, $E_{\mathrm{PE}}^{\mathrm{m}}$ seems to be very low for this element. It is known that the WF for zirconium oxide is much lower than that of zirconium metal (Samsonov 1973). This may be the explanation for the increased SE yield in this case.

Niobium

The results for niobium are shown in Figure 1(m). The SE yield reduces after cleaning especially at low PE energy. There appears to be good agreement between our results and those of Bronshtein and Fraiman (1969). However, from the backscattering results (El-Gomati *et al*. 2008), we know that our Nb sample was oxidized. Hence, we can either conclude that the sample that Bronshtein and Fraiman (1969) used was also oxidized, or that oxidation has little effect on δ for Nb. Septier and Belgarovi (1985) have also measured δ for Nb and their results are generally higher than ours or those of Bronshtein and Fraiman (1969). The calculations of Ding *et al*. (2001) using Equation (4) are much higher than the experimental values from the cleaned specimen.

Molybdenum

The results for molybdenum are shown in Figure 1(n). The SE yield slightly reduces after cleaning especially at low PE energy. As in the case of Nb, our results agree with Bronshtein and Fraiman (1969) despite there being evidence of oxide on the surface (El-Gomati *et al*. 2008). The theoretical estimates of Ding *et al*. (2001) using Equation (4) are slightly higher than the experimental values of the as inserted, particularly at high PE. However,

the Ding *et al*. (2001) results are much higher than our cleaned samples and those of Bronshtein and Fraiman (1969). In addition, at higher PE, the results of Bronshtein and Fraiman (1969) also show a bump at about 2500 eV, again indicative of slightly contaminated surfaces. Our cleaned sample does not show such a bump.

Silver

The results for silver are shown in Figure 1(o). The SE yield slightly increases after cleaning except at low PE energy where there is a slight reduction. The results presented here, those of Bronshtein and Fraiman (1969) and Shimizu (1974) all agree quite closely. However, our determined value of E_p^m is a little lower than these authors. The theoretical estimates of Ding *et al*. (2001) using Equation (5) are in good agreement with experimental results except that their value of E_{PE}^m is slightly lower than the experimentally determined value. When using Equation (4), the calculations of Ding *et al*. (2001) overestimate δ.

Cadmium

The results for cadmium are shown in Figure 1(p). There is little change in δ after cleaning for most PE energies, except for a slight increase at high PE energies. The measurements of Bronshtein and Fraiman (1969) are slightly higher than the present data.

Tin

The results for tin are shown in Figure 1(q). There is little change in δ after cleaning for most PE energies, although there is a decrease at low PE energies. The measurements of Bronshtein and Fraiman (1969) agree quite well with the present data for this element.

Gadolinium

The results for gadolinium are shown in Figure 1(r). There is a significant increase in δ after cleaning for all PE energies except the very lowest. Indeed the value of δ for the as-inserted sample at high PE energy is lower than any other element. After cleaning, the maximum value of δ (δ_m) is approaching 2, which is very high and suggests that the SE yield may have been affected by the presence of an oxide. The backscattered electron data (El-Gomati *et al*. 2008) suggest the presence of an oxide on this element. It is probable that the sample was initially coated in a thick adventitious carbon layer that was removed by the Ar cleaning revealing the underlying oxide layer. It is possible that the overlayer may have been charging for the as-inserted sample, which led to the very low values of δ in this case.

Hafnium

The results for hafnium are shown in Figure 1(s). There is a slight increase in δ after cleaning for PE energies above 500 eV. The maximum yield δ_m is high (it is similar to that of Bronshtein and Fraiman 1969) and it could be owing to an increase in the IMFP of the SEs. However, in this case we would also expect an increase in the energy at which δ_m occurs, but instead it is exceptionally low that suggests other reasons for the high value of δ_m.

The results from the backscattered electron yield show that the Hf sample used to acquire the present data was oxidized. We find δ_m to be high in both Zr and Hf, which is not surprising given their chemical similarity. However, this is in contrast to the results of Bronshtein and Fraiman (1969) who found δ_m to be high in Hf, but low in Zr. The best explanation that can be offered is that Bronshtein and Fraiman (1969) also had an oxidized sample for Hf. Samsonov (1973) shows that the WF of hafnium oxide is much less than pure hafnium, which may explain the high SE yield for this sample.

Tantalum

The results for tantalum are shown in Figure 1(t). There is a decrease in δ after cleaning for PE energies below 1 keV. There is good agreement between the present data of the cleaned sample and that of Bronshtein and Fraiman (1969). Thomas and Pattinson (1969) have measured higher values of δ, peaking at $\delta = 1.3$ at 500 eV. The calculations of Ding *et al*. (2001) using Equation (4) are considerably higher than the measurements.

Tungsten

The results for tungsten are shown in Figure 1(u). There is little change in δ after cleaning. Our results are in close agreement with those of Bronshtein and Fraiman (1969) despite there being evidence of our samples being oxidized. The calculations of Ding *et al*. (2001) using Equation (4) are considerably higher than the measurements.

Platinum

The results for platinum are shown in Figure 1(v). The value of δ increases after cleaning for PE energies above ~400 eV. The present data and that of Bronshtein and Fraiman (1969) are in reasonable agreement, although their results tend to be higher at both low and high PE energy and also show a small bump at about 2500 eV, again indicative of sample contamination. Thomas and Pattinson (1969) have measured higher values of δ, peaking at $\delta = 1.8$ at 600 eV. The results of Ding *et al.* (2001) using Equation (5) are also in reasonable agreement with the measurements.

Gold

The results for gold are shown in Figure 1(w). The value of δ increases after cleaning for PE energies above ~400 eV. The present data and those of Bronshtein and Fraiman (1969) agree quite well, but the energy of the maximum of the SE yield (E_{PE}^{m}) is lower for Bronshtein and Fraiman (1969). The theoretical estimates of Ding *et al.* (2001) using Equation (5) are in particularly good agreement with Bronshtein and Fraiman (1969) at low PE energies whereas using Equation (4) results in values of δ that are much higher than the measured values.

Lead

The results for lead are shown in Figure 1(x). The value of δ increases after cleaning for PE energies above ~400 eV. There is good agreement between the present values and those of Bronshtein and Fraiman (1969).

To understand the wealth of data, we have followed the example of Lin and Joy (2005) and determined the values of E_{PE}^{m} and δ_m for each element for each data source (i.e., the present data, the data

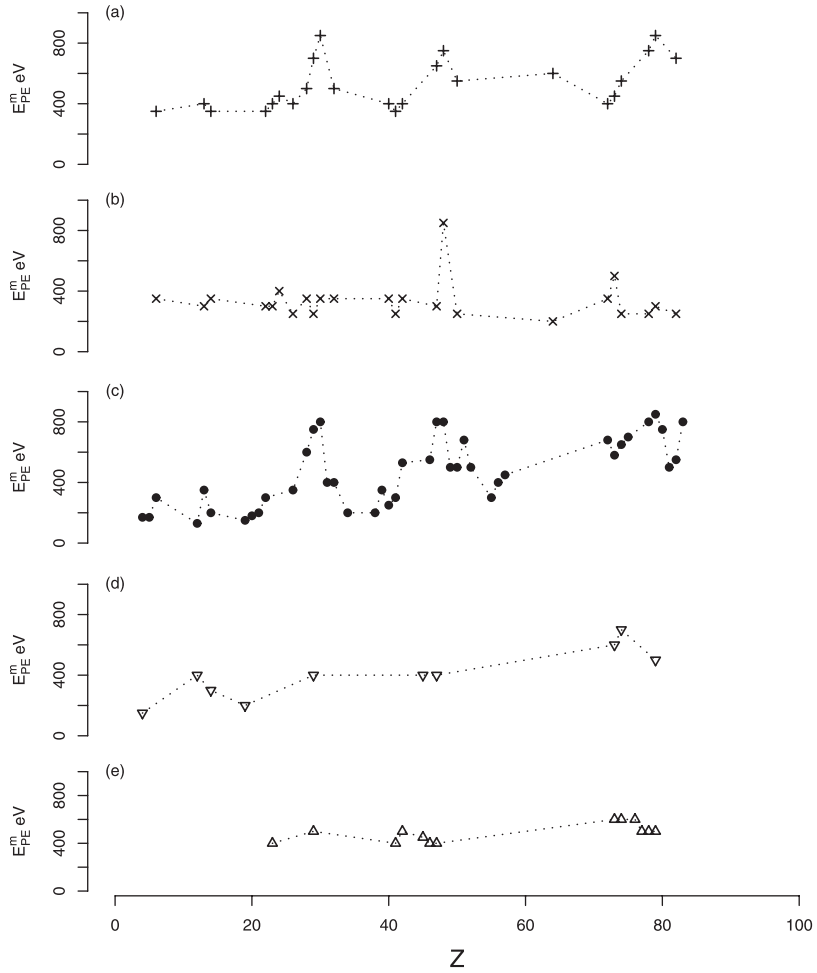

Fig 2. E_{PE}^{m} vs. atomic number, Z, for various different data sets. Data has been offset for clarity. (a) Present data (cleaned), (b) present data (as inserted), (c) Bronshtein and Fraiman (1969), (d) Ding *et al.* (2001) using Equation (5), (e) Ding *et al.* (2001) using Equation (4).

of Bronshtein and Fraiman 1969) and the calculations of Ding *et al.* (2001) using Equations (4) and (5)). A plot of E_{PE}^{m} vs. Z for all data sets can be seen in Figure 2. A similar plot can be found in Bronshtein and Fraiman (1969) (p 154). The as-inserted samples show very little change in the value of E_{PE}^{m} except for cadmium. This element reveals fluctuations in δ with energy (as do many of the as-inserted samples) and it may simply be this that explains the high value of E_{PE}^{m} in this case.

Our results and those of Bronshtein and Fraiman (1969) reveal two separate effects in Figure 2. First, there is a gentle rise in E_{PE}^{m} with atomic number Z. Second, E_{PE}^{m} shows peaks and troughs, the peaks seem to correspond to elements with filled d bands and the troughs correspond to elements at the start of a d band. Plots of δ_m vs. Z (also offset) can be seen in Figure 3. Similar plots to Figure 3 can be found in Bronshtein and Fraiman (1969,p151) and Bronshtein and Fraiman (1962a).

Figure 3 includes data showing how the WF varies with Z for comparison with the values of δ_m. One can see that the Bronshtein and Fraiman (1969) data show increases across the d band similar to the E_{PE}^{m} vs. Z plot (Figure 2) However our data for both as-inserted and cleaned specimens do not show the same correlation. The theoretical simulations of Ding *et al.* (2001) fluctuate, but it is difficult to state that the data show a trend across the d bands. This is owing, in part, to the paucity of the available data. From previous work (El-Gomati *et al.* 2008) it is known that many of our samples were still oxidized after cleaning and this could affect SEE via WF changes or variations in the mean free path of the SEs between the metal and the oxide (Bronshtein and Brozdnichenko 1969).

Monte Carlo Simulations

The MC program used in this work has already been described (El-Gomati *et al.* 2008; Yan *et al.* (1998)). Previous authors have used the imaginary

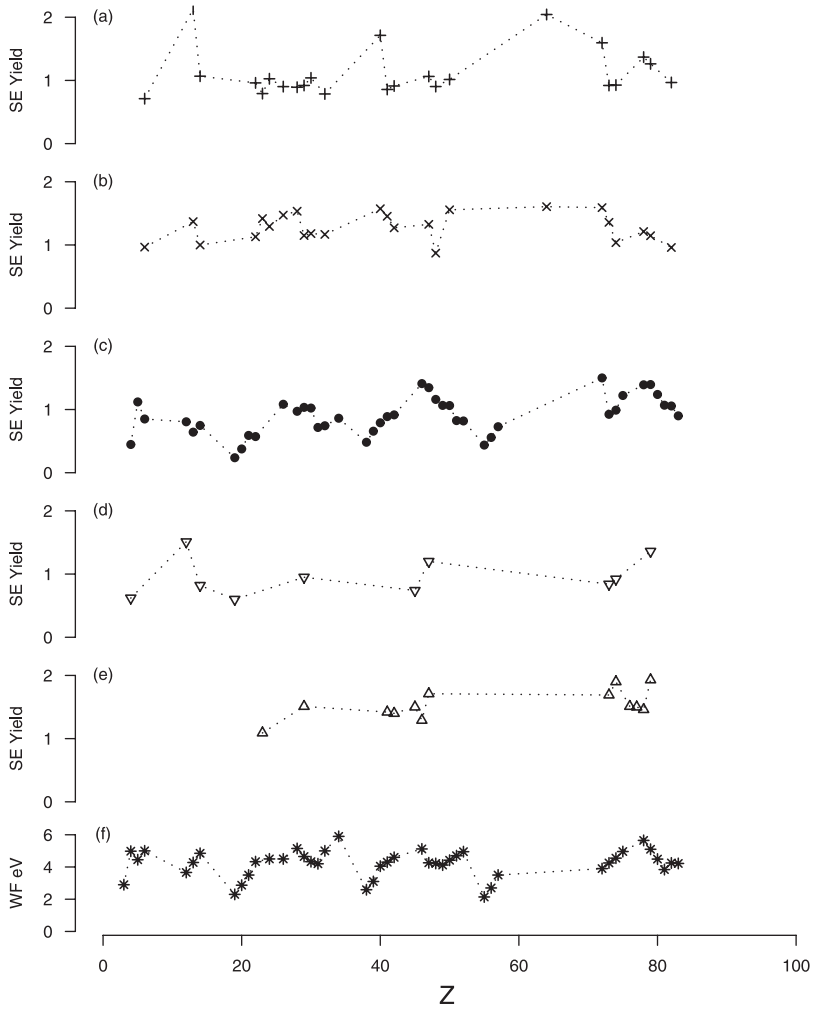

Fig 3. δ_m vs. atomic number Z. (a) Present data (cleaned), (b) present data (as inserted), (c) Bronshtein and Fraiman (1969), (d) Ding *et al.* (2001) using Equation (5), (e) Ding *et al.* (2001) using Equation (4), (f) work functions (WF) of the elements (Weast *et al.* 1985–86).

part of the complex dielectric function to determine the inelastic losses and the electron cascade. However, the relevant functions are only available for some of the elements in this study. Hence, a simpler approach was taken. To provide an estimate of δ, the amount of energy deposited as a function of depth (Equation (1)) was determined for each PE energy (Figure 4). The energy deposited is just the amount of energy lost by each electron as it moves in the material. Care needs to be taken that the energy deposited is equally distributed along the path between each scattering event and not simply attributed to a point half way between each scattering event. The energy deposited can then be translated into the number of electrons generated at each depth, n, by dividing by ε. To remind the reader ε is the energy required to produce a single SE. The number of electrons in each simulation is only 10^4, as the energy deposited along each path between elastic scattering events is recorded, which results in sufficient statistics when only a small number of electrons are simulated.

The histogram of deposited energy vs. depth could then be multiplied by the exponential curve describing the decay of exiting SEs. The rate of decay is controlled by the IMFP of the SEs, λ. The resulting curve is then integrated over depth to arrive at an estimate of δ (Equation (2)). Although this approach does not include the effect of the SE cascade, it is instructive in showing how the changes in the IMFP of the SEs modify the curve of the SE yield vs. PE energy. Koshikawa and Shimizu (1974) found that the depth distribution of SEs does not follow a simple exponential law owing to the cascade process of SEs. The cascade process will tend to increase the yield of SEs generated in the subsurface region. This will give the appearance that the SEs have a longer IMFP than is actually the case.

The electron energy losses are defined by the dielectric function in the MC simulations of Ding *et al.* (2001). The dielectric function does not vary with PE energy in the MC simulations, Hence, one might expect that the form of the curve of δ vs. PE energy will not change by including simulation of the SE cascade. However, the SE cascade grows in amplitude over a small distance and if this distance is similar to the average depth of the PEs, then the SE cascade may not have enough distance to fully grow to its maximum intensity. This effect may influence the value of $E_{\mathrm{PE}}^{\mathrm{m}}$. The fits to our data were carried out using the MC derived estimates of deposited power vs. depth. The MC determinations of $n(z, E)$ were fed into a spreadsheet and Equation (2) was determined numerically within the spreadsheet so that the effect of changing λ on the SE yield could be calculated rapidly. The values of λ are mostly determined by how fast the curves bend downwards at low primary beam energy. Figure 5 shows the determined SE yield curve for Al for several different values of λ. Although it might appear from the figure that $\lambda = 5$ nm is clearly the best fit, one must remember that ε is also a free parameter and so the curves can be freely adjusted up and down. Hence, the curves can all be made to fit the data quite closely despite representing almost 2 orders of magnitude change in λ. Therefore, a small error in the estimate of the stopping power will result in a large change in the estimate of λ. Despite these shortcomings, a fit to the data was undertaken to see if the fitting process at least gave realistic values of λ

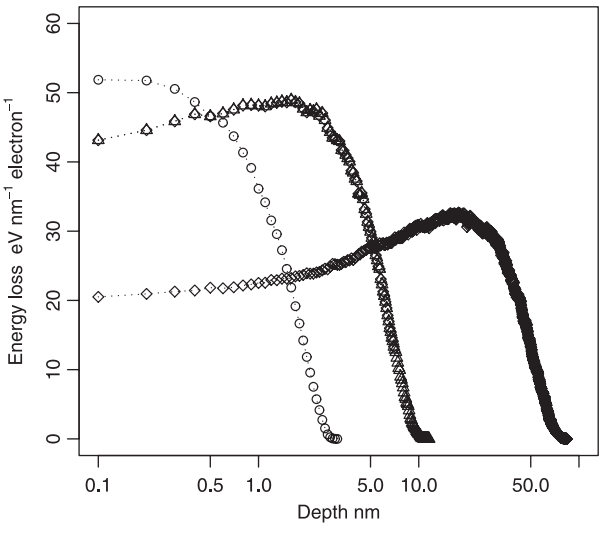

Fig 4. Depth distribution of deposited energy in Al (eV nm^{-1}electron^{-1}) for three different primary beam energies. o = 0.2 keV, Δ = 0.5 keV, $\diamond$ = 2 keV. The abscissa scale is logarithmic to enable the curves to be easily compared.

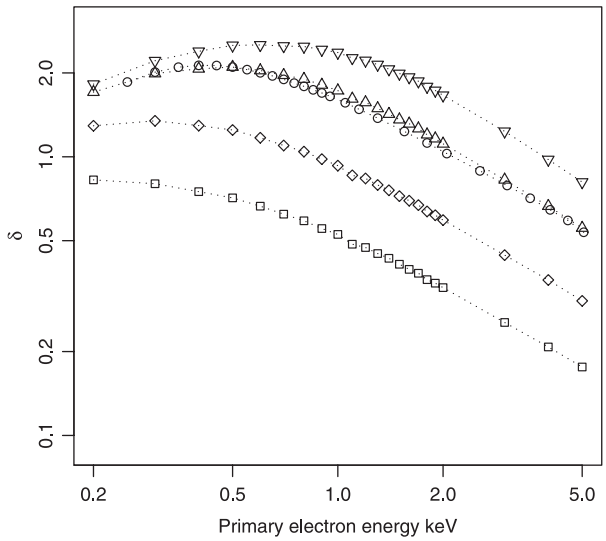

Fig 5. Determined SE yield curves for several different values of λ in Al. o = experimental data, ∇–20 nm, Δ = 5 nm, $\diamond$ = 1 nm, $\square$ = 0.3 nm.

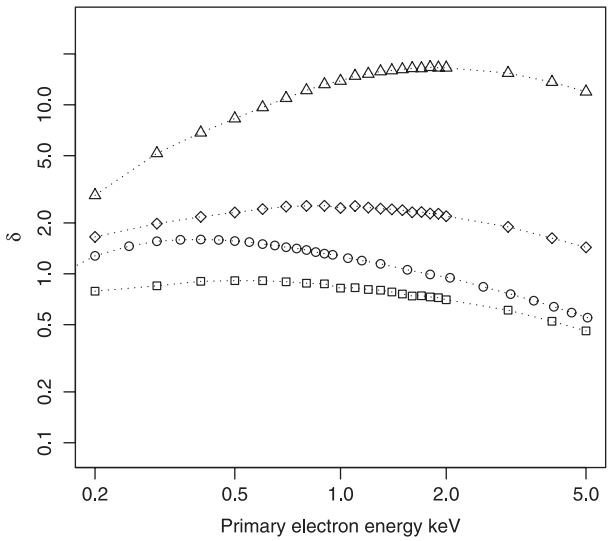

Fig 6. Determined SE yield curves for several different values of λ in Hf. o = experimental data, $\Delta = 2$ nm, $\diamond = 0.5$ nm, $\square = 0.1$ nm. The value of ε has been adjusted so that all curves can be clearly distinguished. By slightly modifying ε, the curve for $\lambda = 0.1$ nm can be made to fit better to the measured curve.

and whether the fits were close to the data, or indicated that the model was insufficient. An example of this is given in Figure 6 where several different values of λ are used to attempt a fit to the experimental data of Hf. The best fit seems to be for a very small value of λ (0.1 nm), although even here the energy of maximum in the SE yield ($E_{\mathrm{PE}}^{\mathrm{m}}$) is distinctly higher than the measured value and the theoretical curve is much flatter than the measured one. The larger values of λ clearly push the maximum in the SE yield too high. Lin and Joy (2005) also report a very low value for λ of 0.2 nm for W (the same as our value for this element).

The estimated values of λ and ε for the elements studied in this report can be seen in Table I. The corresponding values as determined by Lin and Joy (2005) are given for comparison. Most of the determined values of λ are small and in some cases there were poor fits—especially at low λ. This could indicate that the physics behind the model is not accurate. However, there does appear to be a slight increase in λ across each d band.

Lin and Joy (2005) used a similar approach to determine λ (the escape depth of the SEs) and ε (the energy required to produce one SE) to describe δ as a function of PE energy. However, these two parameters are clearly correlated. Hence, attempting to determine these parameters by fitting them to a curve of the SE yield vs. PE energy could result in the properties being apparently correlated as was found by Lin and Joy (2005). It should be emphasized that our fitting process was to determine the best λ and then see what value of ε this gave. We did not allow the two parameters to vary independently while attempting the best fit. This is probably the reason for the poor agreement between our results and those of Lin and Joy (2005).

Table I Estimates of λ and ε taken from the stopping power as a function of depth as determined by MC and adjusting λ and ε to get the best fit by eye

Element	λ nm	ε eV	Quality of fit	λ nm	ε eV
C	0.5	28	Poor	2.5	80
Al	5	120	V. good	1.7	32
Si	1.2	40	Good	2.7	90
Ti	0.4	31	Good	0.5	25
V	0.6	50	Good		
Cr	0.3	25	Good	1.2	47
Fe	0.3	42	Good	0.6	45
Ni	0.3	45	Good	1.0	65
Cu	0.6	63	V. Good	0.6	35
Zn	1.0	70	Medium	2.5	120
Ge	1.0	68	Good	1.0	50
Zr	0.5	22	Medium	0.5	35
Nb	0.3	37	Medium	0.3	20
Mo	0.4	52	Medium	1.0	60
Ag	0.5	39	V. Good	1.0	50
Cd	1.2	84	Medium	1.5	70
Sn	1.0	64	Medium	1.0	43
Gd	1.0	31	Poor		
Hf	0.1	70	Poor	1.0	45
Ta	0.3	41	Poor	0.7	60
W	0.2	30	Poor	0.2	20
Pt	0.6	63	Medium	0.5	30
Au	1.0	82	Medium	0.5	35
Pb	0.8	52	Medium	0.8	40

The corresponding data as determined by Lin and Joy (2005) are shown in the last two columns.

Discussion

The as-inserted samples in our study tended to show fluctuations in δ with PE energy. On cleaning, the curves tended to be much smoother. However, it is known from the backscattering measurements on the same samples that many of the cleaned surfaces studied in this report were still oxidized (El-Gomati *et al.* 2008). This presence of oxide is known to change the IMFP of the SEs in the case of Al (Bronshtein and Brozdnichenko 1969) or modify the WF. Bronshtein and Fraiman (1969) used *in-situ* evaporation techniques to achieve clean surfaces (Bronshtein and Segal 1960a, b) and indeed Bronshtein and Fraiman (1969) show that the δ_{m} vs. Z plots are quite similar to the variation of the WF vs. Z (Figure 3) in agreement with the theoretical work of Baroody (1950). However, the anomalously high value that Bronshtein and Fraiman (1969) obtained for δ_{m} for

Hf suggests that they too had a slightly oxidized sample in this case.

According to Dionne (1975), the value of E_{PE}^{m} is dependent on the bulk and is not affected by the condition of the surface. This implies that the plots of E_{PE}^{m} vs. Z remain unaffected by oxidation as long as the oxide layer is thin enough. Hence, Figure 2 reveals a d band filling effect owing to the properties of the bulk metal despite the oxidized nature of the surfaces.

Why does the number of electrons in the d band influence the shape and height of the SE yield δ? The most probable reason is that the IMFP of the SEs is increasing as the number of d electrons increases. This will increase the number of electrons available to be excited from the bulk. In addition, as the depth of penetration of the PEs increases with PE energy, then δ should increase with PE energy to greater PE values when the SE IMFP is long. This will result in a higher value for E_{PE}^{m} that causes the peaks seen in Figure 2 for the elements Zn, Cd and Au. The role of the d band in low energy electron scattering has been explored by Siegmann (1994) who measured the IMFP for Cu, Ag and Au. However, the energy of the electrons in his experiment was lower than the energy of the SEs in this report. In a theoretical study, Drouhin (1997) explored the mean free path of low-energy electrons and found that the scattering rate is dependent on the number of holes in the d bands. Zarate *et al.* (1999) extended this work and found that the free electron scaling of the lifetime $(E\text{-}E_F)^{-2}$ is modified to $(E\text{-}E_F\text{-}\omega_d)^{-2}$ where ω_d is the energy difference between the Fermi energy and the top of the d band. Table II shows ω_d calculated for the 3d series from data given by Sigalas *et al.* (1992). Clearly ω_d decreases as the d band fills. This will lead to longer lifetimes for the elements with more d electrons. Zhukov *et al.* (2006) have used GW+T *ab initio* calculations to determine the lifetimes and path lengths of low-energy electrons in Fe, Ni, Pt and Au.

TABLE II The energy difference (in eV) between the top of the d band and the Fermi level for the 3d transition metals (as calculated from Sigalas et al. 1992)

Element	ω_d bcc	ω_d fcc
Ca	4.73	
Sc	4.46	4.41
Ti	4.33	4.14
V	3.89	6.20
Cr	2.69	2.98
Mn	2.35	2.11
Fe	1.50	1.44
Co	1.02	0.64
Ni	0.068	0.23
Cu	−1.41	−1.31
Zn	−7.25	−6.95

However, the range of electron energies they explore is below that typical of SEE. As the MC results of Ding *et al.* (2001) do not reveal the changes in the values of δ_m and E_{PE}^{m} across the d bands, then one can conclude that the IMFP they use for the SEs does not change significantly across the d bands. As they use dielectric functions from optical measurements to determine the IMFP of the SEs, one can conclude that the dielectric functions they use do not appear to provide good estimates of the IMFP of SEs (i.e., electrons ~1–5 eV above the vacuum level). A better approach might be to use *ab initio* determined values of the IMFP (Sorini *et al.* 2006).

Although a shorter IMFP can be explained in terms of d band filling, it still does not explain the poor fit of our MC model to the experimental data from Hf and other d band elements. One possible explanation is that the efficiency of the SE cascade (which has not been modelled) varies with PE energy (i.e., ε varies with E_{PE}). The efficiency of the cascade could be affected in two ways. First, the cascade will amplify as the electrons travel through the material, which requires a certain distance to create this amplification. If the initial SE is too close to the surface, then perhaps SE cascade will not be as strong as a cascade that had been initiated at a slightly greater depth. This is in accord with the work of Koshikawa and Shimizu (1973) who found that the SE emission does not follow a simple exponential decay law for SE escaping from the surface. In addition, the effective atomic number Z_{eff} that the PE feels from an atom in the sample will reduce as the primary energy reduces, thus reducing the capacity for generating SEs.

Chen *et al.* (2007) carried out Reflection Electron Energy Loss Spectroscopy (REELS) experiments on Mo and Ta surfaces. They found that the surface plasmon loss is considerably enhanced especially at low PE energy. The surface plasmons decay and produce SEs in the same manner as the bulk plasmons. The varying intensity with PE energy is consistent with our observations of δ being inconsistent with our MC calculations. The very short IMFP of the SE that the curves for Hf, Ta and W in Figure 1 imply are consistent with a large surface plasmon contribution to the SE emission. The presence of oxygen on these surfaces will no doubt influence the REELS spectrum and in turn the form of the SEE curves in Figure 1. If one wishes to model these surfaces using MC following the approach of Ding *et al.* (2001), then the electron energy loss functions for the surface plasmons will need to be taken into account. The current approach of using the complex dielectric function to model the electron energy losses is applicable only for bulk energy losses.

The results of Ding *et al.* (2001) are in good agreement with the measured results when one takes the assumption that the starting energy of the SE is determined by a distribution of energies in the valence band (Equation (5)). Using the approach that the electrons at the Fermi level are the source of the SEs (Equation (4)) results in predicted SE yields larger than the experimentally determined curves. The E_{PE}^{m} vs. Z plots for the MC results of Ding *et al.* (2001) show a gradual rise consistent with the contribution of backscattered electrons on δ. However, there is no evidence of the d band filling effect-causing peaks in the curve of δ vs. atomic number at Cu, Ag and Au. Similarly, the theoretically determined (using Ding *et al.* 2001) plots of δ_m vs. Z also show no correlation with WF or trends along the d bands. However, if the appropriate SE IMFP and surface plasmon contributions were added to the computer model, it is likely these effects would become apparent in the MC simulations.

Conclusions

Much of the variation in δ between many different authors can be attributed to contamination/oxidation of the sample surfaces. The form of the curve of the energy of the maximum in δ (i.e., E_{PE}^{m}) vs. primary energy (PE) is less dependent on surface oxidation than a plot of δ_m vs. PE and reveals a dependence on the filling of the d levels. This dependence can be explained as an increase in the inelastic mean free path (IMFP of the secondary energy (SEs)) with the number of electrons in the d band. This is consistent with theoretical predictions of the lifetime and scattering rates of low-energy electrons in transition metals. It also shows a gradual increase in the energy of the maximum in δ with atomic number, which can be attributed to the contribution of backscattering to δ.

Monte Carlo (MC) simulations by Ding *et al.* (2001) do not reveal the same variations in SE yield curves across the d bands. From this one can determine that the IMFP of the SEs is not accurately replicated in these simulations. This is probably owing to the use of the dielectric function (which was used to determine the IMFP of the SEs) not being an accurate method for determining the transport properties of low-energy electrons in the range $\sim$1–5 eV above the vacuum level.

MC simulations carried out in this report suggest that the IMFP of the SEs in some elements (e.g., Hf, Ta, W) are anomalously short. This could be explained if the surface plasmons contribute significantly to the SE yield.

The secondary electron emission (SEE) as found in scanning electron microscopy (SEMs) is largely dependent on the surface layer of adsorbed or chemisorbed elements referred to as "crud." Removing the surface layer would (in many circumstances) reveal new sources of contrast, but would be dominated by effects induced by oxidation for certain metals (e.g., Al, Zr, Hf). Given the normal vacuum conditions in a typical SEM, a surface cannot be made to be entirely clean for most metals. Simulating the SEM images in a computer would need to take these effects into account and indeed the data we present need to be taken into consideration when interpreting low voltage scanning electron microscopy (LVSEM) images.

Acknowledgements

The authors would like to thank Prof. J.A.D. Matthew for useful discussions and Y. Sakarov for his assistance in translating sections of Bronshtein and Fraiman (1969). The members of the Physics and Electronics Workshop have created much of the excellent equipment used in this work. The work was funded by the EPSRC.

References

Assa'd AM: The effect of energetic backscattering electrons in quantitative multi-spectral analysis. D. Phil. thesis, University of York, (1995).

Baroody EM: A theory of secondary electron emission from metals. *Phys Rev* **78**, 780–787 (1950).

Barut AO: The mechanism of secondary electron emission. *Phys Rev* **93**, 981–984 (1954).

Bongeler R, Golla U, Kussens M, Reimer L, Schendler B, *et al*: Electron-specimen interactions in low-voltage scanning electron microscopy. *Scanning* **15**, 1–18 (1993).

Bronshtein IM, Brozdnichenko AN: Secondary electron emission from aluminum oxide. *Radio Eng Electron Phys* **14**, 1801–1803 (1969).

Bronshtein IM, Denisov SS: Inelastic scattering of electrons in solids with the primary beam at oblique incidence. *Sov Phys Solid State* **6**, 2106–2110 (1965a).

Bronshtein IM, Denisov SS: Effect of the work function on parameters of secondary electron emission. *Sov Phys Solid State* **6**, 1515–1518 (1965b).

Bronshtein IM, Fraiman BS: Secondary emission properties of metals and semiconductors and the periodic system of elements. *Sov Phys Solid State* **3**, 2337–2339 (1962a).

Bronshtein IM, Fraiman BS:Secondary electron emission from some solid bodies. *Sov Phys Solid State* **3**, 2087–2088 (1962b).

Bronshtein IM, Fraiman BS: Vtorichnaya Elektronnaya Emissiya (secondary electron emission) Nauka-Moskva (1969).

Bronshtein IM, Segal RB: An investigation of electron reflection from certain metals. *Sov Phys Solid State* **1**, 1142–1145 (1960a).

Bronshtein IM, Segal RB: Inelastic scattering of electrons and secondary electron emission in certain metals I. *Sov Phys Solid State* **1**, 1365–1496 (1960b).

Bruining H, De Boer JM: Secondary electron emission part 1. Secondary electron emission of metals. *Physica* **5**, 17–30 (1938).

Chen T, Zhang ZM, Ding ZJ, Shimizu R, Goto K: Effective energy loss functions of Mo and Ta derived from reflection electron energy loss spectra. *J Electron Spectrosc Relat Phenom* **159**, 62–65 (2007).

Dekker AJ: Secondary electron emission. *Solid State Phys* **6**, 251 (1958).

Ding ZJ, Tang XD, Shimizu R: Monte Carlo study of secondary electron emission. *J Appl Phys* **89**, 718–726 (2001).

Dionne GF: Origin of secondary electron emission yield curve parameters. *J Appl Phys* **46**, 3347–3351 (1975).

Drouhin H-J: Low-energy electron mean free path and its spin dependence in transition metals. *Phys Rev B* **56**, 14886–14889 (1997).

El-Gomati MM, Walker CGH, Assa'd AMD, Zadražil M: Theory experiment comparison of the electron backscattering factor from solids at low electron energy (250–5,000 eV). *Scanning* **30**, 2–15 (2008).

El-Gomati MM, Wells TCR: Very low-energy electron microscopy of doped semiconductors. *Appl Phys Lett* **79**, 2931–2933 (2001).

Johnson JB, McKay KG: Secondary electron emission from germanium. *Phys Rev* **93**, 668–672 (1954).

Joy DC: "A Database of electron solid interactions" Revision ♯04-02, [The complete database, containing tabulations of all available data sets as well as a comprehensive bibliography, can be downloaded as a Microsoft Word document from http://web.utk.edu/~srcutk/htm/interact.htm] (2006).

Kanter H: Contribution of backscattered electrons to secondary electron formation. *Phys Rev* **121** 681–684 (1961).

Koshikawa T, Shimizu R: Secondary electron and backscattering measurements for polycrystalline copper with a spherical retarding-field analyzer. *J Phys D Appl Phys* **6**, 1369–1380 (1973).

Koshikawa T, Shimizu R: A Monte Carlo calculation of low-energy secondary electron emission from metals. *J Phys D: Appl Phys* **7**, 1303–1315 (1974).

Kuhr JC: Monte Carlo Simulation der sub-keV-Elektronstreuung für Anwendungen in der Elektronmikroskopie und Elektronspektroskopie, Thesis, Universität Rostock (1998).

Kuhr J-Ch, Fitting H-J: Monte Carlo Simulation of low energy electron scattering in solids. *Phys State Solid (A)* **172**, 433–449 (1999).

Lin Y, Joy DC: A new examination of secondary electron yield data. *Surf Interface Anal* **37**, 895–900 (2005).

Luo S, Zhang X, Joy DC: Experimental determination of electron stopping powers at low energies. *Radiat Eff Defects Solids* **117**, 235–242 (1991).

McKay KG: Secondary Electron Emission. Recent Advances in Electronics Vol. 1, Academic Press, New York, 65 (1948).

Ohya K: Comparative study of target atomic number dependence of ion induced and electron induced secondary electron emission. *Nucl Instrum Methods Phys Res B* **206**, 52–56 (2003).

Penn DR: Electron mean-free-path calculations using a model dielectric function. *Phys Rev B* **35**, 482–486 (1987).

Reimer L: Scanning Electron Microscopy, Springer Verlag, Berlin Heidelberg (1985).

Samsonov GV: The Oxide Handbook, Plenum, New York (1973).

Septier A, Belgarovi M: Secondary electron emission yields of carbon coated copper and niobium real surfaces. *IEEE Trans Electr Insulators* **EI-20**, 725. (1985).

Shimizu R: Secondary electron yield with primary electron beam of kilo-electron-volts. *J Appl Phys* **45**, 2107–2111 (1974).

Siegmann HC: Recent results of cross-fertilization between electron spectroscopy and magnetism. *J Electron Spectrosc Relat Phenom* **68**, 505–514 (1994).

Sigalas M, Papaconstantopolous PA, Bacalis NC: Total energy and band structure of the 3d, 4d and 5d metals. *Phys Rev B* **45**, 5777–5783 (1992).

Sorini AP, Kas JJ, Rehr JJ, Prange MP, Levine ZH: Ab initio calculations of electron inelastic mean free paths and stopping powers. *Phys Rev B* **74**, 165111 (2006).

Streitwolf HW: Zur Theorie der Sekundärelektronenemission von Metallen Der Anregungsprozeß. *Annu Phys* **458**, 183–196 (1959).

Thomas S, Pattinson EB: Automatic measurement of secondary electron emission characteristics of TaC, TiC and ZrC. *J Phys D: Appl Phys* **2–2**, 1539–1547 (1969).

Thomas S, Pattinson EB: Range of electrons and contribution of back-scattered electrons in secondary production in aluminium. *J Phys D: Appl Phys* **3**, 349–357 (1970).

Wagner LF, Spicer WE: Photoemission study of the effect of bulk doping and oxygen exposure on silicon surface states. *Phys Rev B* **9**, 1512–1515 (1974).

Weast RC, Astle MJ, Beyer WH (Eds.): CRC Handbook of Chemistry and Physics 66th ed., CRC press, Boca Raton, FL (1985–1986).

Whetten NR: Methods in Experimental Physics Vol. IV, Academic Press, NY (1962).

Yan H, El-Gomati MM, Prutton M, Wilkinson DK, Chu DP, *et al.*: Mc3D: a three-dimensional Monte Carlo system simulating image contrast in surface analytical scanning electron microscopy I—object oriented software design and tests. *Scanning* **20**, 465–484 (1998).

Zadrazil M: Noncharging scanning electron microscopy, Ph.D. thesis, Technical University of Brno, Czech Republic (2002).

Zarate E, Apell P, Echenique PM: Calculation of low-energy electron lifetimes. *Phys Rev B* **60**, 2326–2332 (1999).

Zhukov VP, Chulkov EV, Echenique PM: Lifetimes and inelastic mean free path of low-energy excited electrons in Fe, Ni, Pt, and Au: ab initio GW+T calculations. *Phys Rev B* **73**, 125105 (2006).

Ziaja B, London RA, Hajdu J: Unified model of secondary electron cascades in diamond. *J Appl Phys* **97**, 064905 (2005).

Ziaja B, London RA, Hajdu J: Ionization by impact electrons in solids: electron mean free path fitted over a wide energy range. *J Appl Phys* **99**, 033514 (2006).